

University of Bergen, Department of Physics
Scientific/Technical Report No. 1995-02
ISSN 0803-2696
hep-ph/9502283
July, 2018

Testing CP in the Bjorken process

Arild Skjold
Per Osland

Section for Theoretical Physics
Department of Physics*
University of Bergen
Allégt. 55, N-5007 Bergen, Norway

Abstract

In a more general electroweak theory, there could be Higgs particles that are odd under CP , and also Higgs-like particles which are not eigenstates of CP . We discuss distributions which for the Bjorken process are sensitive to the CP parity. Correlations among momenta of the initial electron and final-state fermions yield this kind of information. We discuss also observables which may demonstrate presence of CP violation and identify a phase shift δ which is a measure of the strength of CP violation in the Higgs-vector-vector coupling, and which can be measured directly in the decay distribution. We present Monte Carlo data on the expected efficiency, and conclude that it is relatively easy to determine whether the produced particle is even or odd under CP . However, observation of any CP violation would require a very large amount of data.

*Electronic mail addresses: {skjold,osland}@vsfys1.fi.uib.no

1 Introduction

One of the main purposes of accelerators being planned and built today, is to elucidate the mechanism of mass generation. In the Standard Model mass is generated via an $SU(2)$ Higgs doublet, associated with the existence of a Higgs particle, whereas in more general models there are typically several such Higgs fields, and also more physical particles.

Another fundamental issue is the origin of CP violation. While this question will be studied in considerable detail at the SLAC B-Factory and at other dedicated B -physics experiments, there is of course the possibility that CP violation may be related to the Higgs sector, as first suggested by Weinberg [1]. Therefore, when some Higgs candidate is discovered, it will be important to determine its properties under CP .

In the context of Higgs production via the Bjorken mechanism [2], we shall here consider how angular distributions may serve to disentangle a scalar Higgs candidate from a pseudoscalar one. In trying to probe the uniqueness of the scalar character of the Higgs boson as provided by the Standard Model, we have to confront its predictions with those provided by possible extensions of the Standard Model. Next, by allowing for CP violation in the Higgs sector, we briefly discuss some possible signals of such effects. While the Standard Model induces CP violation in the Higgs sector at the one-loop level provided the Yukawa couplings contain both scalar and pseudoscalar components [3], we actually have in mind an extended model, such as e.g., the two-Higgs-doublet model [4].

Below we postulate an effective Lagrangian which contains CP violation in the Higgs sector. In cases considered in the literature, CP violation usually appears as a one-loop effect. This is due to the fact that the CP -odd coupling introduced below is a higher-dimensional operator and in renormalizable models these are induced only at loop level. Consequently we expect the effects to be small and the confirmation of presence of CP violation to be equally difficult. CP non-conservation has manifested itself so far only in the neutral kaon system. In the context of the Standard Model this CP violation originates from the Yukawa sector via the CKM matrix [5]. Although there may be several sources of CP violation, including the mixing matrix, we will here consider a simple model where the CP violation is restricted to the Higgs sector and in particular to the coupling between

some Higgs boson and the vector bosons. Specifically, by assuming that the coupling between the Higgs boson H and the Z has both scalar and pseudoscalar components, the most general coupling for the HZZ -vertex relevant for the Bjorken process may be written as [6, 7]

$$i 2^{5/4} \sqrt{G_F} \left[m_Z^2 g^{\mu\nu} + \xi(k_1^2, k_2^2) (k_1 \cdot k_2 g^{\mu\nu} - k_1^\mu k_2^\nu) + \eta(k_1^2, k_2^2) \epsilon^{\mu\nu\rho\sigma} k_{1\rho} k_{2\sigma} \right], \quad (1.1)$$

with k_j the vector boson momentum, $j = 1, 2$. The first term is the familiar CP -even $Z^\mu Z_\mu H$ tree-level Standard Model coupling. The second term stems from the dimension-5 CP -even operator $Z^{\mu\nu} Z_{\mu\nu} H$ with $Z_{\mu\nu} = \partial_\mu Z_\nu - \partial_\nu Z_\mu$. The last term is CP odd and originates from the dimension-5 operator $\epsilon^{\mu\nu\rho\sigma} Z_{\mu\nu} Z_{\rho\sigma} H$. Simultaneous presence of CP -even and CP -odd terms leads to CP violation, whereas presence of only the last term describes a pseudoscalar coupling to the vector bosons. The higher-dimensional operators are radiatively induced and we may therefore safely neglect the contribution from the second term. This is due to the fact that CP -violating effects always arise from interferences and since loops in the Standard Model are already suppressed, we conclude that only new CP -violating effects that interfere with Standard Model tree amplitudes are potentially significant. The strength parameter η may in general be complex, with $\text{Im } \eta$ describing the absorptive part of the amplitude arising from final-state interactions.

Related studies have been reported by [6, 7, 8, 9] in the context of how to discriminate CP eigenstates. However it should be noted that our study takes advantage of the azimuthal angular distributions similar to the correlations between decay planes involving scalar and pseudoscalar Higgs bosons [10], including Monte Carlo data on the expected efficiency. In the context of CP violation, related studies have been reported by [7].

2 Distinguishing CP eigenstates

We compare here the production of a Standard-Model Higgs ($h = H$) with the production of a ‘pseudoscalar’ Higgs particle ($h = A$) via the Bjorken mechanism,

$$e^-(p_1) e^+(p_2) \rightarrow f(q_1) \bar{f}(q_2) h(q_3). \quad (2.1)$$

The couplings of H and A to the vector bosons are given by retaining only the first and last term in (1.1), respectively.

Let the momenta of the two final-state fermions and the initial electron (in the overall $c.m.$ frame) define two planes, and denote by ϕ the angle between those two planes (see eq. (2.8) below). Then we shall discuss the angular distribution of the cross section σ ,

$$\frac{1}{\sigma} \frac{d\sigma}{d\phi} \quad (2.2)$$

both in the case of CP -even and CP -odd Higgs bosons.

The fermion-vector couplings are given by g_V and g_A . As a parameterization of these, we define the angles χ by

$$g_V \equiv g \cos \chi, \quad g_A \equiv g \sin \chi. \quad (2.3)$$

In the present work, the only reference to these angles is through $\sin 2\chi$ (see table 1 of ref. [10]). The differential cross section can then be written as

$$d^5\sigma_h = \frac{G_F N_1}{2\sqrt{2}s} D(s, s_1) W_h d\text{Lips}(s; q_1, q_2, q_3), \quad h = H, A, \quad (2.4)$$

with \sqrt{s} the $c.m.$ energy and $d\text{Lips}(s; q_1, q_2, q_3)$ denoting the Lorentz-invariant phase space. Furthermore, N_1 is a colour factor, which is three for quarks, and one for leptons. The momentum correlations are in the massless fermion approximation given by

$$\begin{aligned} W_H &= X_+ - \sin 2\chi \sin 2\chi_1 X_-, \\ W_A &= \frac{|\eta(s, s_1)|^2}{m_Z^4} \left[-2X_-^2 + \frac{1}{4} s s_1 (Z_1 - \sin 2\chi \sin 2\chi_1 Z_2) \right], \end{aligned} \quad (2.5)$$

with $\sin 2\chi$ and $\sin 2\chi_1$ referring to the initial and final fermions, respectively, and where

$$\begin{aligned} X_{\pm} &= (p_1 \cdot q_1)(p_2 \cdot q_2) \pm (p_1 \cdot q_2)(p_2 \cdot q_1), \\ Z_1 &= [(p_1 \cdot q_1) + (p_2 \cdot q_2)]^2 + [(p_1 \cdot q_2) + (p_2 \cdot q_1)]^2 - \frac{1}{2} s s_1, \\ Z_2 &= [(p_1 + p_2) \cdot (q_1 - q_2)][(p_1 - p_2) \cdot (q_1 + q_2)]. \end{aligned} \quad (2.6)$$

The normalization in eq. (2.4) involves the function

$$D(s, s_1) = m_Z^4 \frac{g_1^2}{(s_1 - m_Z^2)^2 + m_Z^2 \Gamma_Z^2} \frac{g_2^2}{(s - m_Z^2)^2 + m_Z^2 \Gamma_Z^2}, \quad (2.7)$$

with

$$s \equiv (p_1 + p_2)^2, \quad s_1 \equiv Q^2 \equiv (q_1 + q_2)^2.$$

Finally, m_Z and Γ_Z denote the mass and total width of the Z boson, respectively.

We first consider angular correlations of two planes, one spanned by the incident electron momentum (\mathbf{p}_1) and that of the final-state vector boson (\mathbf{Q}), and the other one spanned by the two final-state fermions (\mathbf{q}_1 and \mathbf{q}_2). Hence, we define the angle ϕ by

$$\cos \phi = \frac{(\mathbf{p}_1 \times \mathbf{Q}) \cdot (\mathbf{q}_1 \times \mathbf{q}_2)}{|\mathbf{p}_1 \times \mathbf{Q}| |\mathbf{q}_1 \times \mathbf{q}_2|}. \quad (2.8)$$

Integrating the Higgs production cross section (2.4) over the polar angle of the vector boson (or Higgs) momentum, as well as over the way the energy is shared between the two fermions, we find

$$\frac{d^2\sigma_h}{d\phi ds_1} = \frac{N_1}{144\sqrt{2}(4\pi)^4} \frac{G_F}{s^2} \sqrt{\lambda(s, s_1, m^2)} D(s, s_1) W'_h, \quad h = H, A, \quad (2.9)$$

with azimuthal distributions given by the expressions

$$\begin{aligned} W'_H &= \lambda(s, s_1, m^2) + 12ss_1 + 2ss_1 \cos 2\phi \\ &\quad + \sin 2\chi \sin 2\chi_1 \left(\frac{3\pi}{4}\right)^2 \sqrt{ss_1} (s + s_1 - m^2) \cos \phi, \\ W'_A &= \frac{|\eta(s, s_1)|^2}{m_Z^4} \lambda(s, s_1, m^2) 2ss_1 \left(1 - \frac{1}{4} \cos 2\phi\right), \end{aligned} \quad (2.10)$$

and where $\lambda(x, y, z) \equiv x^2 + y^2 + z^2 - 2(xy + xz + yz)$ is the Källén function. The term Z_2 of eq. (2.5) vanishes under the integration over the polar angle referred to above, and does not contribute in eq. (2.10). It would contribute to the forward-backward (with respect to the beam axis) asymmetry of the Higgs cross section.

A more inclusive distribution is obtained if we integrate over the invariant mass of the final state fermion pair. Thus, let us consider

$$\frac{d\sigma_h}{d\phi} = \int_0^{(\sqrt{s}-m)^2} ds_1 \frac{d^2\sigma_h}{d\phi ds_1}. \quad (2.11)$$

The distributions of eq. (2.2) take the form

$$\frac{2\pi}{\sigma_H} \frac{d\sigma_H}{d\phi} = 1 + \alpha(s, m) \cos \phi + \beta(s, m) \cos 2\phi, \quad (2.12)$$

$$\frac{2\pi}{\sigma_A} \frac{d\sigma_A}{d\phi} = 1 - \frac{1}{4} \cos 2\phi. \quad (2.13)$$

We shall consider the case when the energy is large enough to allow both the Higgs and the Z decaying to fermions to be on their mass shells. We may then use the narrow-width approximation, effectively setting $s_1 = m_Z^2$, so that

$$\begin{aligned}\alpha(s, m) &= \sin 2\chi \sin 2\chi_1 \left(\frac{3\pi}{4}\right)^2 \frac{\sqrt{s} m_Z (s + m_Z^2 - m^2)}{\lambda(s, m_Z^2, m^2) + 12s m_Z^2}, \\ \beta(s, m) &= \frac{2s m_Z^2}{\lambda(s, m_Z^2, m^2) + 12s m_Z^2}.\end{aligned}\tag{2.14}$$

At very high energies, $\lambda(s, m_Z^2, m^2) \sim s^2$, and the coefficients $\alpha(s, m)$ and $\beta(s, m)$ will vanish as $s^{-1/2}$ and s^{-1} , respectively. Therefore, the Standard-Model distribution (2.12) will asymptotically become flat, whereas the CP -odd distribution in eq. (2.13) is independent of energy and Higgs mass. A representative set of angular distributions is given in fig. 1 for the case $e^+e^- \rightarrow \mu^+\mu^-h$ for both LEP2 and higher energies, and for different Higgs masses. (With ϕ being defined as the angle between two oriented planes, it can take on values $0 \leq \phi \leq 2\pi$.) Due to the $\sin 2\chi$ -factors in eq. (2.14), $\alpha/\beta \simeq 0.1$ for the case of e.g. muons in the final state. This explains why the $\cos\phi$ contribution from eq. (2.12) is strongly suppressed in fig. 1. There is seen to be a clear difference between the CP -even and the CP -odd cases.

Experimentally, however, one faces the challenge of contrasting two angular distributions with a restricted number of events and allowing also for background. We shall here focus on the intermediate Higgs mass range; more specifically, we consider $m \lesssim 140$ GeV where the Higgs decays dominantly to $b\bar{b}$. The main background will then stem from $e^+e^- \rightarrow ZZ$ and also $e^+e^- \rightarrow Z\gamma, \gamma\gamma$. The cleanest channel for isolating the Higgs signal from the background is provided by the $\mu^+\mu^-$ and e^+e^- decay modes of the Z boson.

Let us next limit consideration to the energy range $\sqrt{s} = 300 - 500$ GeV, as appropriate for a linear collider [11], henceforth denoted NLC. We impose the reasonable cuts and constraints described in [8]; e.g. $|m_{\mu^+\mu^-} - m_Z| \leq 6$ GeV and $|\cos\theta_Z| \leq 0.6$, where $m_{\mu^+\mu^-}$ denotes the invariant mass of the muon pair and $\cos\theta_Z$ is the angle between \mathbf{p}_1 and \mathbf{Q} given in eq. (2.8). The signal for $e^+e^- \rightarrow ZH \rightarrow \mu^+\mu^-b\bar{b}$ will then be larger than the background $e^+e^- \rightarrow ZZ \rightarrow \mu^+\mu^-b\bar{b}$ by an order of magnitude. In the following we shall thus neglect the background in the discussion of (2.12) versus (2.13). With $\sigma(e^+e^- \rightarrow ZH) \sim 200$ fb and an integrated luminosity of 20 fb^{-1} a year [8], about 4000

Higgs particles will be produced per year, in this intermediate mass range. However, following [8] we have only ~ 30 signal events $e^+e^- \rightarrow ZH \rightarrow \mu^+\mu^-b\bar{b}$ left per year for e.g. a NLC operating at $\sqrt{s} = 300$ GeV and a Higgs particle of mass $m = 125$ GeV. In the case $e^+e^- \rightarrow ZH \rightarrow e^+e^-b\bar{b}$ we also have a t-channel background contribution from the ZZ fusion process $e^+e^- \rightarrow e^+e^-(ZZ) \rightarrow e^+e^-H$. This contribution may be neglected at LEP energies, but it is comparable to the s-channel contribution at higher energies. However, this contribution can be suppressed by imposing a cut on the invariant mass of the final-state electrons, e.g. $|m_{e^+e^-} - m_Z| \leq 6$ GeV. Hence, we can effectively treat the electrons on the same footing as the muons, thereby obtaining a doubling of the event rate.

Imposing the cut $|\cos\theta_Z| \leq b$, the predictions for the azimuthal correlations of eqs. (2.12)–(2.13) get modified. For the CP -even case we find

$$\begin{aligned}\alpha^b(s, m) &= \sin 2\chi \sin 2\chi_1 \left(\frac{3\pi}{4}\right)^2 \frac{\sqrt{s} m_Z (s + m_Z^2 - m^2)}{\xi(b)\lambda(s, m_Z^2, m^2) + 12s m_Z^2} \zeta(b), \\ \beta^b(s, m) &= \frac{2\xi(b)s m_Z^2}{\xi(b)\lambda(s, m_Z^2, m^2) + 12s m_Z^2},\end{aligned}\tag{2.15}$$

with

$$\begin{aligned}\xi(b) &= \frac{1}{2}(3 - b^2), \quad \xi(1) = 1, \\ \zeta(b) &= \frac{2}{\pi} \left(\frac{\frac{\pi}{2} - \arccos b}{b} + \sqrt{1 - b^2} \right), \quad \zeta(1) = 1,\end{aligned}\tag{2.16}$$

whereas for the CP -odd case

$$-\frac{1}{4} \rightarrow -\frac{\xi(b)}{3 + b^2}.\tag{2.17}$$

In order to demonstrate the potential of the NLC for determining the CP of the Higgs particle, we show in fig. 2 the result of a Monte Carlo simulation. For this purpose we have used PYTHIA [12], suitably modified to allow for the CP -odd case. The statistics correspond to 3 years of running¹ using both the $\mu^+\mu^-$ and e^+e^- decay modes of the Z boson. This yields about 200 events in these channels. As already stated, the α in (2.14) is small, and although the cut $b = 0.6$ makes α increase as shown in (2.15), the $\cos\phi$

¹The event rate is based on the Standard Model, and could be different for a non-standard Higgs sector.

term is still too small to show up in the Monte Carlo simulation. For $\sqrt{s} = 300$ GeV and $m_H = 125$ GeV, the ‘bare’ prediction (2.14) for β is 0.12, but the cut $b = 0.6$ increases it slightly to 0.14. Similarly, the ‘-1/4’ of (2.13) changes significantly to -0.39. Consequently, the cut makes it easier to discriminate between the CP -even distribution and the CP -odd one. From fig. 2 we see that the individual angular Monte Carlo distributions are consistent with the predictions, showing that a three-year data sample is large enough to reproduce the azimuthal distributions. In the Standard-Model case the fit gives 0.92 ± 0.07 and 0.2 ± 0.1 for the predictions 1.00 and 0.14, respectively, with $\chi^2 = 1.0$. In the CP -odd case the fit gives 0.94 ± 0.07 and -0.4 ± 0.1 for the predictions 1.00 and -0.39 , respectively, with $\chi^2 = 0.7$. More importantly, it is possible to verify the scalar nature of the Standard-Model Higgs after about 3 years of running at the NLC since the coefficient of the $\cos 2\phi$ term is more than 4 standard deviations away from the corresponding coefficient for the $CP = -1$ case. Using likelihood ratios, as described in [13], for choosing between the two hypotheses of CP even and CP odd, we find that less than 3 years of running suffices if we require a discrimination by four standard deviations.

An alternative test has recently been suggested by Arens et. al. [14] in the context of Higgs decaying via vector bosons to four fermions, where one studies the energy spectrum of one of the final-state fermions. Applying this idea to the Bjorken process one would study the energy distribution of an outgoing fermion, e.g. μ^- or e^- . Introducing the scaled lepton energy, $x = 4E_{l^-}/\sqrt{s}$, $l = \mu, e$, we shall consider the energy distribution of the cross section with respect to this final-fermion energy,

$$\frac{1}{\sigma} \frac{d\sigma}{dx} \quad (2.18)$$

both in the case of CP -even and CP -odd Higgs bosons. In the narrow-width approximation we find

$$\frac{1}{\sigma_H} \frac{d\sigma_H}{dx} = \frac{3s^2}{4\sqrt{\lambda}(\lambda + 12sm_Z^2)} \left[4m_Z^2 + 2(s + m_Z^2 - m^2)x - sx^2 \right], \quad (2.19)$$

$$\frac{1}{\sigma_A} \frac{d\sigma_A}{dx} = \frac{3s^2}{8\lambda^{3/2}} \left[\left(2\frac{\lambda}{s} + 4m_Z^2 \right) - 2(s + m_Z^2 - m^2)x + sx^2 \right], \quad (2.20)$$

where $\lambda = \lambda(s, m_Z^2, m^2)$. The range in x is given by $x_- \leq x \leq x_+$, with

$$sx_{\pm} = s + m_Z^2 - m^2 \pm \sqrt{\lambda} \quad (2.21)$$

In this case there is a non-trivial dependence on the *c.m.* energy and the Higgs mass, also for the *CP*-odd case. A representative set of energy distributions is given in fig. 3 for the case $e^+e^- \rightarrow \mu^+\mu^-h$ for both LEP2 and NLC energies. There is seen to be a clear difference between the *CP*-even and the *CP*-odd cases. Before we turn to the Monte-Carlo simulations, we shall impose the cut $|\cos\theta_Z| \leq b$, as in the case of angular correlations. This cut modifies eq. (2.19) so that

$$\begin{aligned} \frac{1}{\sigma_H^b} \frac{d\sigma_H^b}{dx} &= \frac{3s^2}{2\sqrt{\lambda} [\xi(b)\lambda + 12s m_Z^2]} \left\{ 2m_Z^2 \left(b^2 - \frac{3s m_Z^2}{\lambda} (1 - b^2) \right) \right. \\ &\quad \left. + \left[(s + m_Z^2 - m^2) x - \frac{s}{2} x^2 \right] \left(\xi(b) + \frac{3s m_Z^2}{\lambda} (1 - b^2) \right) \right\}, \quad (2.22) \end{aligned}$$

whereas the *CP*-odd distribution is independent of any cut in $\cos\theta_Z$. Of course the total cross section scales with b .

In fig. 4 we show the result of a Monte-Carlo simulation for the energy distribution eq. (2.18) analogous to the one in fig. 2. For $\sqrt{s} = 300$ GeV and $m_H = 125$ GeV, the coefficients in (2.19) and (2.20) are 0.3, 1.3, -0.7 and 1.5, -2.1 , 1.1, respectively, for increasing powers of x . If we impose the cut $|\cos\theta_Z| \leq 0.6$, the Standard-Model predictions are changed to -0.003 , 2.0, -1.1 . Hence, as in the case of angular distributions, the cut makes it easier to discriminate between the *CP*-even distribution and the *CP*-odd one. In the Standard-Model case the fit gives 1.7 ± 0.2 and -0.9 ± 0.1 for the predictions 2.0 and -1.1 , respectively, with $\chi^2 = 1.0$. Naturally, the fit is not sensitive to the first coefficient. In the *CP*-odd case the fit gives 1.6 ± 0.3 , -2.2 ± 0.7 , and 1.1 ± 0.4 for the predictions 1.5, -2.1 and 1.1, respectively, with $\chi^2 = 0.6$. Also in this case a three-year data sample is enough to reproduce the predicted energy distributions. An analysis of the likelihood ratios demonstrates that less than 3 years of running is sufficient if we require the correct answer with a discrimination by four standard deviations, but more events seem to be required than in the case of angular distributions.

3 CP violation

As previously mentioned, if we allow for both the Standard-Model and the CP -odd term in the Higgs-vector coupling (1.1), then there will be CP violation. This situation will be discussed here. It is similar to the case of Higgs decay discussed elsewhere [15]. We discard the higher-dimensional CP -even term for the reasons stated in the Introduction.

The differential cross section can then be written as [cf. (2.4)–(2.7)]

$$d^5\sigma = \frac{G_F N_1}{2\sqrt{2}s} D(s, s_1) \left[W_H + \frac{\text{Re } \eta}{m_Z^2} W_1 + \frac{\text{Im } \eta}{m_Z^2} W_2 + W_A \right] d\text{Lips}(s; q_1, q_2, q_3). \quad (3.1)$$

The new momentum correlations are in the massless-fermion approximation given by

$$\begin{aligned} W_1 &= -\epsilon_{\alpha\beta\gamma\delta} p_1^\alpha p_2^\beta q_1^\gamma q_2^\delta [Y_- - \sin(2\chi) \sin(2\chi_1) Y_+], \\ W_2 &= (\sin 2\chi + \sin 2\chi_1) Y_1 - (\sin 2\chi - \sin 2\chi_1) Y_2, \end{aligned} \quad (3.2)$$

where

$$\begin{aligned} Y_{\mp} &= (p_1 \mp p_2) \cdot (q_1 \mp q_2), \\ Y_1 &= [(p_2 \cdot q_1) - (p_1 \cdot q_2)] [(p_1 \cdot p_2) (q_1 \cdot q_2) + (p_1 \cdot q_2) (p_2 \cdot q_1) - (p_1 \cdot q_1) (p_2 \cdot q_2)], \\ Y_2 &= [(p_1 \cdot q_1) - (p_2 \cdot q_2)] [(p_1 \cdot p_2) (q_1 \cdot q_2) - (p_1 \cdot q_2) (p_2 \cdot q_1) + (p_1 \cdot q_1) (p_2 \cdot q_2)] \end{aligned} \quad (3.3)$$

The term W_2 of eq. (3.1), like Z_2 of eq. (2.5), vanishes under integration over the polar angle.

The distribution corresponding to (2.9)–(2.10) can be written compactly as

$$\begin{aligned} \frac{d^2\sigma}{d\phi ds_1} &= \frac{N_1}{144\sqrt{2}(4\pi)^4} \frac{G_F}{s^2} \sqrt{\lambda(s, s_1, m^2)} D(s, s_1) \\ &\times \left[\lambda(s, s_1, m^2) + 4ss_1 (1 + 2\rho^2) + 2ss_1 \rho^2 \cos 2(\phi + \delta) \right. \\ &\left. + \sin 2\chi \sin 2\chi_1 \left(\frac{3\pi}{4} \right)^2 \sqrt{ss_1} (s + s_1 - m^2) \rho \cos(\phi + \delta) \right] + \mathcal{O}((\text{Im } \eta)^2) \end{aligned} \quad (3.4)$$

with a modulation function

$$\rho = \sqrt{1 + (\text{Re } \eta)^2 \lambda(s, s_1, m^2) / (4m_Z^4)}, \quad (3.5)$$

and an angle

$$\delta = \arctan \frac{\text{Re } \eta(s, s_1) \sqrt{\lambda(s, s_1, m^2)}}{2m_Z^2}, \quad -\pi/2 < \delta < \pi/2, \quad (3.6)$$

describing the relative shift in the angular distribution of the two planes, due to CP violation. This rotation vanishes at the threshold for producing a real vector boson (where $\lambda = 0$) and, even for a fixed value of $\text{Re } \eta$, grows with energy (because of the $\sqrt{\lambda}$ -factor). As discussed in the Introduction, the contribution from terms of order $(\text{Im } \eta)^2$ may safely be neglected. However, the compact result (3.4) is valid for any $\text{Re } \eta$. We will comment on how to probe $\text{Im } \eta$ later.

This relation (3.6) can be inverted to give for the CP -odd term in the coupling:

$$\text{Re } \eta = \frac{2m_Z^2}{\sqrt{\lambda(s, s_1, m^2)}} \tan \delta. \quad (3.7)$$

This result (3.4) is completely analogous to the one encountered for the decay of Higgs particles, eq. (12) of [15], if we interchange ϕ and $\pi - \phi$.

Above threshold for producing a real vector meson accompanying the Higgs particle, we may integrate over s_1 in the narrow-width approximation. Imposing the cut $|\cos \theta_Z| \leq b$, the distribution of eq. (2.2) takes the compact form

$$\frac{2\pi}{\sigma^b} \frac{d\sigma^b}{d\phi} = 1 + \alpha^{b'}(s, m) \rho \cos(\phi + \delta) + \beta^{b'}(s, m) \rho^2 \cos 2(\phi + \delta), \quad (3.8)$$

with

$$\begin{aligned} \alpha^{b'}(s, m) &= \sin 2\chi \sin 2\chi_1 \left(\frac{3\pi}{4}\right)^2 \frac{\sqrt{s} m_Z (s + m_Z^2 - m^2) \zeta(b)}{\lambda(s, m_Z^2, m^2) [\xi(b) + (3 + b^2) s (\text{Re } \eta)^2 / 2m_Z^2] + 12s m_Z^2}, \\ \beta^{b'}(s, m) &= \frac{2s m_Z^2 \xi(b)}{\lambda(s, m_Z^2, m^2) [\xi(b) + (3 + b^2) s (\text{Re } \eta)^2 / 2m_Z^2] + 12s m_Z^2}, \end{aligned} \quad (3.9)$$

and ρ and δ given by eqs. (3.5) and (3.6), substituting $s_1 = m_Z^2$.

Any CP violation would thus show up as a ‘‘tilt’’ in the azimuthal distribution, by the amount δ . The amount could be extracted from a measurement of either of the ‘‘odd’’ coefficients A' or B' in

$$\frac{2\pi}{\sigma^b} \frac{d\sigma^b}{d\phi} = 1 + A(s, m) \cos \phi + B(s, m) \cos 2\phi + A'(s, m) \sin \phi + B'(s, m) \sin 2\phi \quad (3.10)$$

along the lines suggested in [15].

A representative set of angular distributions is given in fig. 5 for a broad range of $\text{Re } \eta$ values. We have considered a Higgs boson of $m = 200$ GeV accompanied by a

$\mu^+\mu^-$ -pair in the final state, produced at $\sqrt{s} = 500$ GeV. We observe that for $\text{Re } \eta \lesssim 0.1$ and $\text{Re } \eta \gtrsim 5$, the deviations from the CP -even and CP -odd distributions, respectively, are small. Experimentally it will be very difficult to disentangle two distributions which differ by such a small phase shift. This should be compared with the situation in fig. 1 and fig. 2.

We note that the special cases $\eta = 0$ and $|\eta| \gg 1$ correspond to the CP even and CP odd eigenstates, respectively. Hence, the distribution (3.8) should be interpreted as being intermediate between those for the two eigenstates; see fig.5.

In order to see how one can extract the dependence on the term proportional to $\text{Im } \eta$, let us now turn to a discussion of energy asymmetries. We multiply the differential cross section eq. (3.1) with the weighted energy difference $(\omega_1 - \omega_2) / (\omega_1 + \omega_2)$ for the two final fermions before integrating over energies. This energy-weighted differential cross section corresponding to eq. (3.4) takes the form

$$\begin{aligned} \frac{d^2\tilde{\sigma}}{d\phi ds_1} &= \frac{\text{Im } \eta}{m_Z^2} \frac{N_1 \sin 2\chi_1}{36\sqrt{2}(4\pi)^4} \frac{G_F \lambda^{3/2}(s, s_1, m^2)}{s} \frac{s_1 D(s, s_1)}{s + s_1 - m^2} \\ &\times \left[1 + \frac{\sin 2\chi}{2 \sin 2\chi_1} \left(\frac{3\pi}{16} \right)^2 \frac{s + s_1 - m^2}{\sqrt{ss_1}} \cos \phi \right], \end{aligned} \quad (3.11)$$

since, in this case, only the W_2 -term in (3.1) gives a non-vanishing contribution. The energy-weighted differential cross section makes no reference neither to the CP -even nor to the CP -odd results, but is proportional to $\text{Im } \eta$ which describes the absorptive part of the amplitude. A study of the above asymmetry thus allows us to probe for final state interactions and CP violation in the Bjorken process.

4 Summary and concluding remarks

We have addressed the problem of estimating the amount of data needed in order to distinguish a scalar Higgs from a pseudoscalar one at a future linear collider. We have argued that this is most likely not possible at LEP2. However, we have demonstrated that one will be able to establish the scalar nature of the Higgs boson at the Next Linear Collider from an analysis of angular and energy correlations. This study has been carried

out for the case $\sqrt{s} = 300$ GeV, $m = 125$ GeV. Similar results are expected in other cases as long as the background is small. In cases where the background can not be significantly suppressed a more dedicated study would be required.

In order to establish or rule out specific models, one will also need to compare different branching ratios, in particular to fermionic final states. The methods proposed above instead deal with quite general properties of the models.

It is a pleasure to thank Anne Grete Frodesen, Per Steinar Iversen, Conrad Newton and Torbjörn Sjöstrand for helpful discussions. This research has been supported by the Research Council of Norway.

References

- [1] S. Weinberg, *Phys. Rev. Lett.* 37 (1976) 657.
- [2] J. D. Bjorken, in *Proceedings of the 1976 SLAC Summer Institute on Particle Physics*, ed. M. Zipf (SLAC Report No. 198, 1976) p. 22;
B.L. Ioffe and V.A. Khoze, *Sov. J. Part. Nucl.* 9 (1978) 50;
D.R.T. Jones and S.T. Petcov, *Phys. Lett.* 84B (1979) 440;
J. Finjord, *Physica Scripta* 21 (1980) 143.
- [3] S. Weinberg, *Phys. Rev. Lett.* 63 (1989) 2333;
Phys. Rev. D 42 (1990) 860.
- [4] T.D. Lee, *Phys. Rev. D* 8 (1973) 1226.
- [5] N. Cabibbo, *Phys. Rev. Lett.* 10 (1963) 531;
M. Kobayashi and T. Maskawa, *Prog. Theor. Phys.* 49 (1973) 652.
- [6] J. R. Dell'Aquila and C. A. Nelson, *Phys. Rev. D* 33 (1986) 101.
- [7] D. Chang, W. -Y. Keung and I. Phillips, *Phys. Rev. D* 48 (1993) 3225.
- [8] V. Barger, K. Cheung, A. Djouadi, B.A. Kniehl and P.M. Zerwas, *Phys. Rev. D* 49 (1994) 79.

- [9] B. Grządkowski and J.F. Gunion, UCD preprint 95-5, hep-ph/9501339.
- [10] A. Skjold and P. Osland, Phys. Lett. B311 (1993) 261.
- [11] B.H. Wiik, in *HEP 93*, Proc. Int. Europhysics Conference on High Energy Physics, Marseille, 22–28 July, 1993 eds. J. Carr and M. Perrottet (Editions Frontieres, Gif-sur-Yvette, 1994) p. 739.
- [12] T. Sjöstrand, Computer Physics Commun. 82 (1994) 74.
We use PYTHIA version 5.702 and JETSET version 7.404.
- [13] B.P. Roe, *Probability and Statistics in Experimental Physics*, (Springer-Verlag Inc., New York, 1992).
- [14] T. Arens, U. D. J. Gieseler and L. M. Sehgal, Phys. Lett. B339 (1994) 127,
T. Arens and L. M. Sehgal, PITHA 94/37, hep-ph/9409396, September 1994.
- [15] A. Skjold and P. Osland, Phys. Lett. B329 (1994) 305.

Figure captions

- Fig. 1. Angular distributions of the planes defined by incoming e^- and final-state fermions for a CP -even Higgs particle (solid) compared with the corresponding distribution for a CP -odd one (dashed). Different energies and masses are considered in the CP -even case. We assume $\sqrt{s} = 200$ and 500 GeV at LEP2 and NLC, respectively. The considered values of the Higgs mass at the LEP2 are 70 and 100 GeV, and at the NLC 125 and 200 GeV. In the CP -odd case there is no dependence neither on energy nor on Higgs mass
- Fig. 2. Monte Carlo data displaying the angular distribution of events $e^+e^- \rightarrow ZH \rightarrow l^+l^-b\bar{b}$, $l = \mu, e$ for a Standard-Model Higgs versus a CP-odd one. We have taken $\sqrt{s} = 300$ GeV, $m = 125$ GeV, and an angular cut $|\cos\theta| \leq b = 0.6$.
- Fig. 3. Characteristic distributions for the scaled energy of the l^- , $l = \mu, e$ in the Bjorken process $e^+e^- \rightarrow l^+l^-h$. Different energies and masses are considered.
- Fig. 4. Monte Carlo data displaying the lepton energy distribution for events $e^+e^- \rightarrow ZH \rightarrow l^+l^-b\bar{b}$, $l = \mu, e$ for a Standard-Model Higgs versus a CP-odd one. We have taken $\sqrt{s} = 300$ GeV and $m = 125$ GeV.
- Fig. 5. Characteristic angular distributions for different amounts of CP violation, including the CP -even ($\eta = 0$) and CP -odd ($|\eta| \gg 1$) eigenstates. We have used $\text{Re } \eta = 0.1, 0.5, 5$ for $\sqrt{s} = 500$ GeV and $m = 200$ GeV.

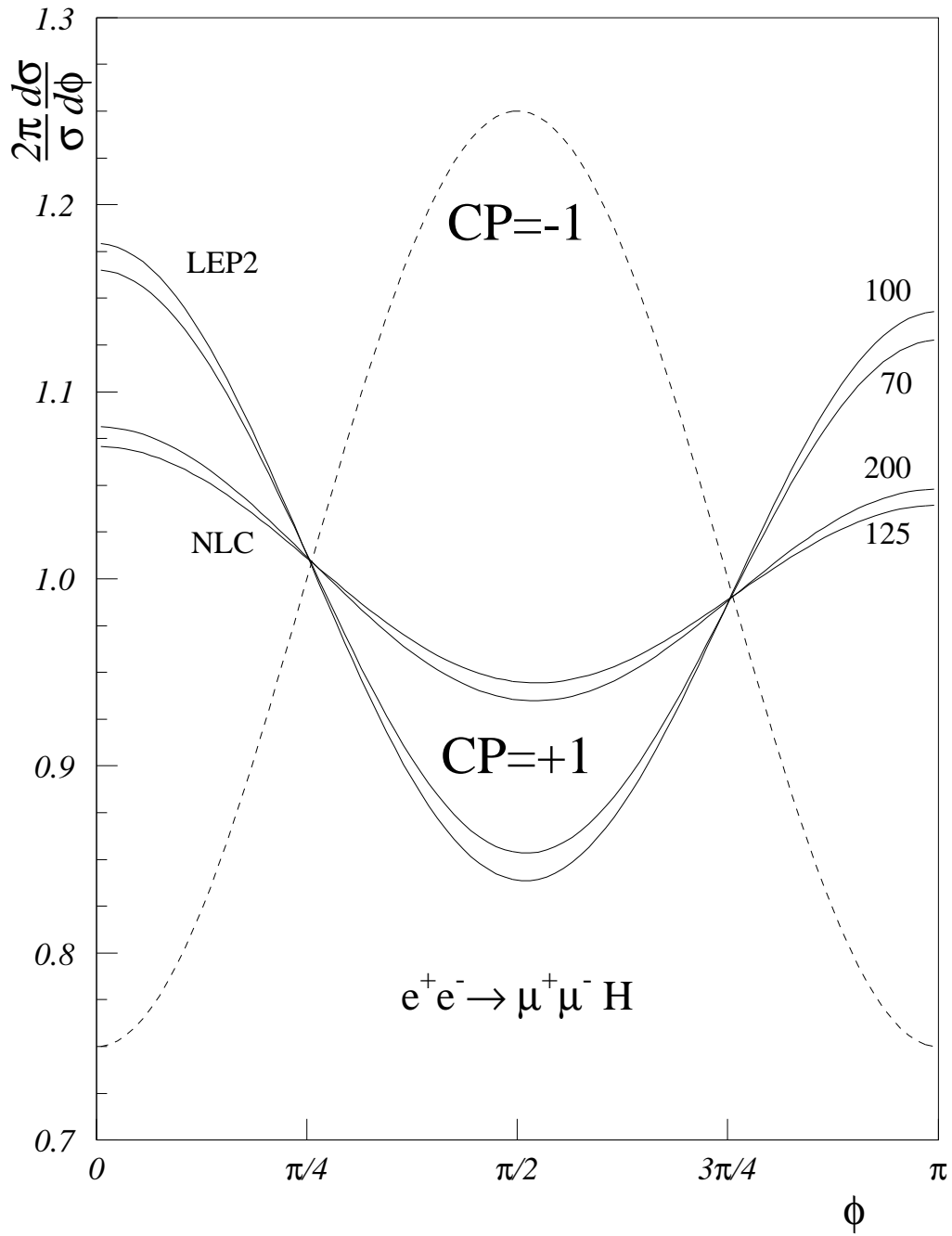


Figure 1

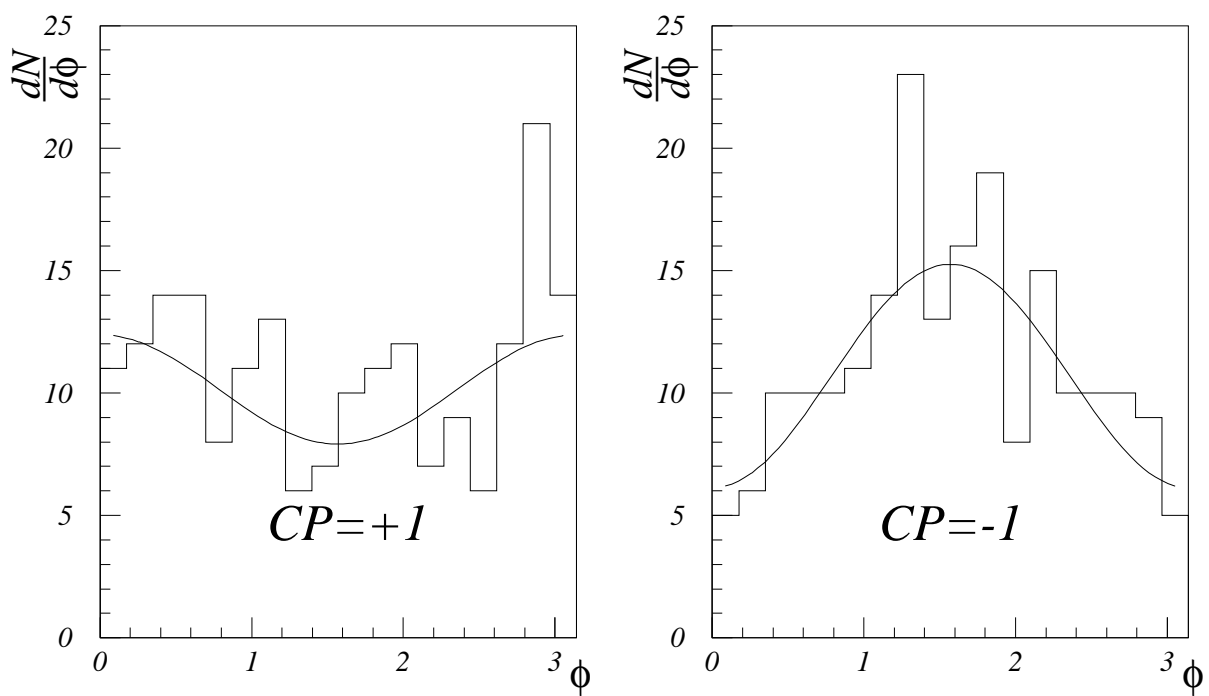


Figure 2

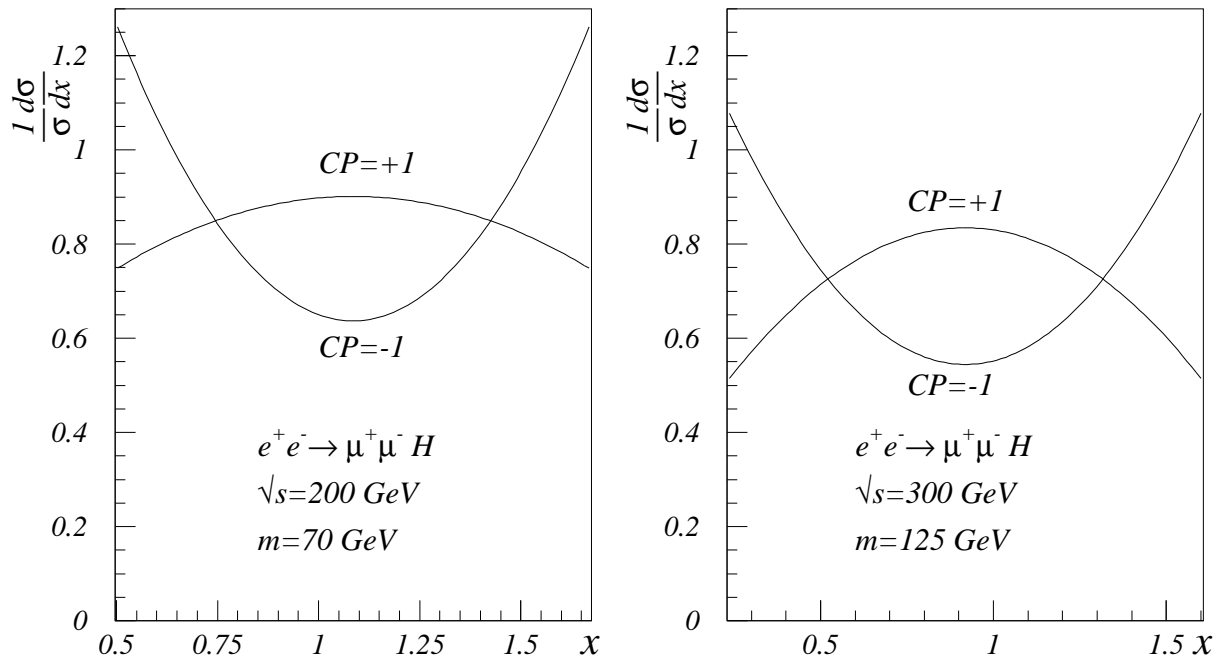


Figure 3

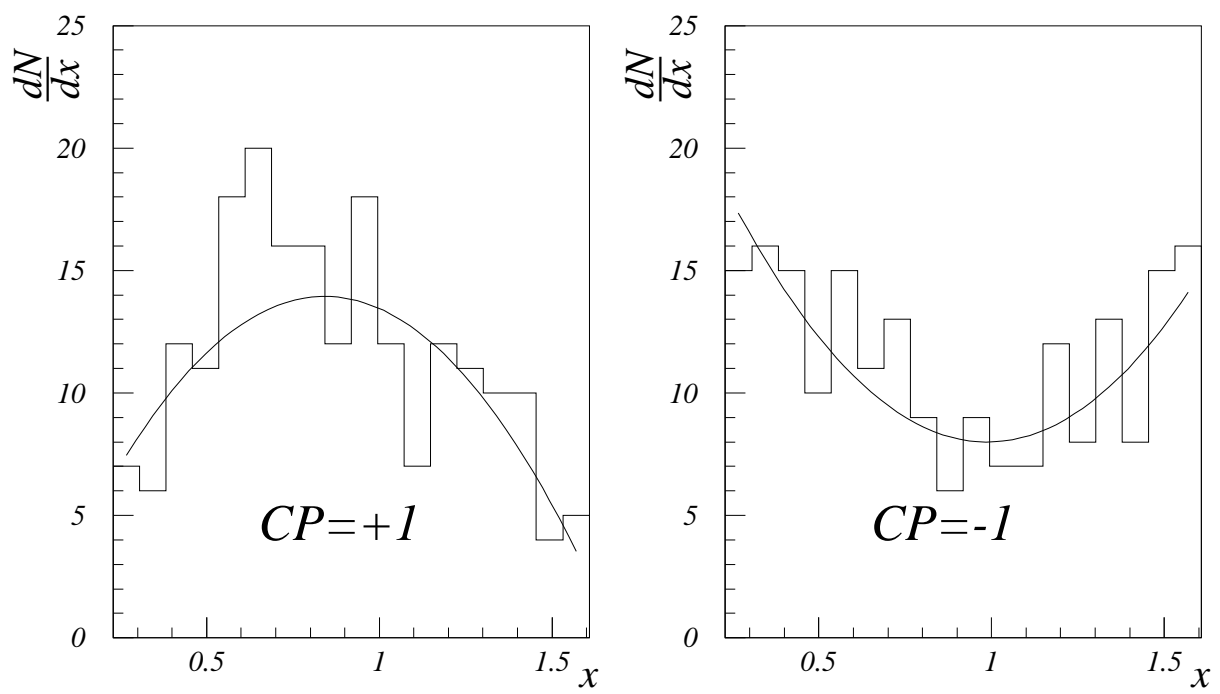
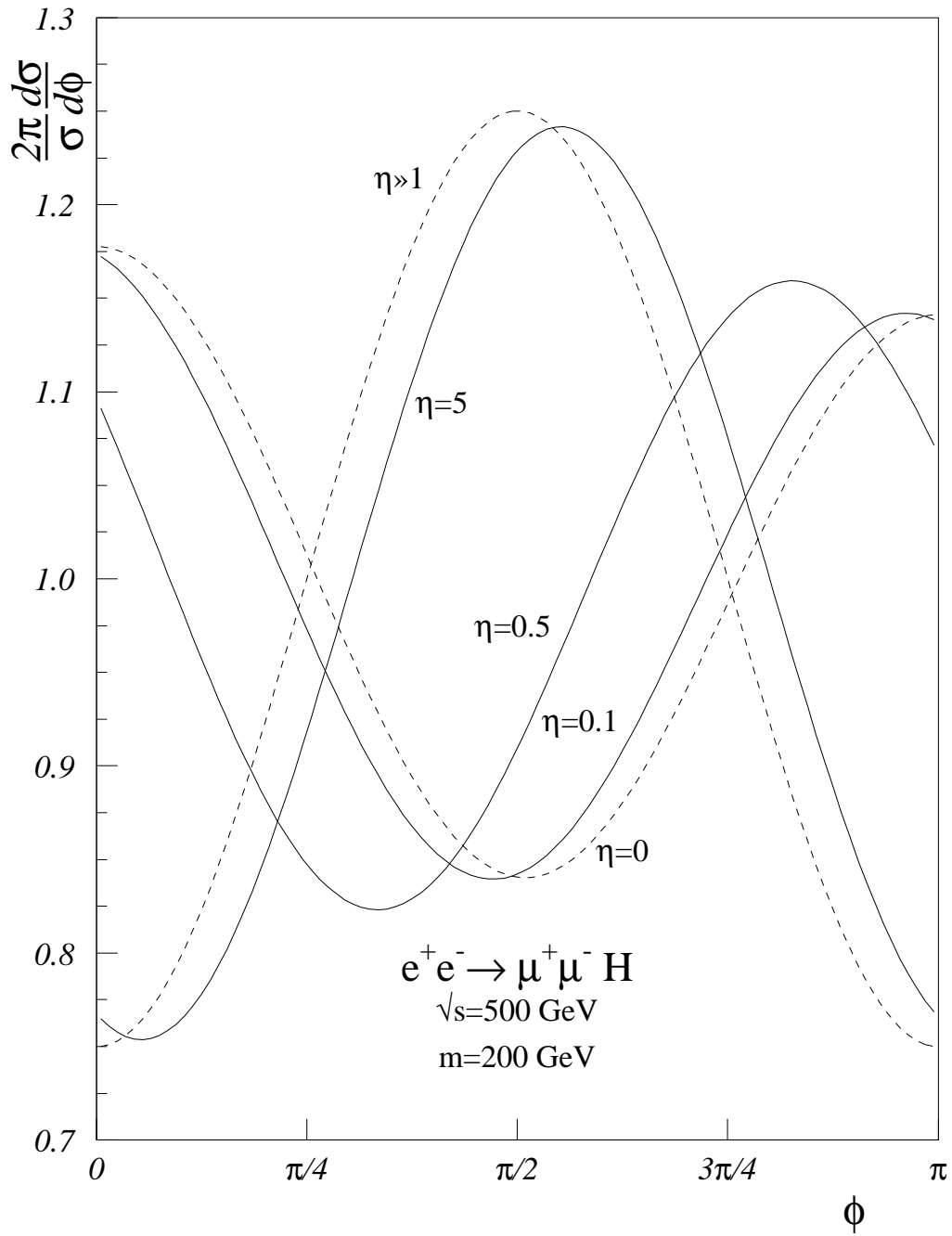


Figure 4



20
Figure 5